Creation and Dynamical Co-evolution of Electron and Ion Channel Transport Barriers*

D.E. Newman
Department of Physics, University of Alaska at Fairbanks, Fairbanks, Alaska, USA

B. A. Carreras
Oak Ridge National Laboratory, Oak Ridge, Tennessee 37831, U. S. A.

Daniel Lopez-Bruna
Asociación Euratom-CIEMAT, Madrid, Spain

P.W. Terry
Univ. of Wisconsin, Madison, WI, U. S. A.

Abstract.

A wide variety of magnetic confinement devices have found transitions to an enhanced confinement regime. Simple dynamical models have been able to capture much of the dynamics of these barriers however an open question has been the disconnected nature of the electron thermal transport channel sometimes observed in the presence of a standard ion channel barrier. By adding to simple barrier model an evolution equation for electron fluctuations we can investigate the interaction between the formation of the standard ion channel barrier and the somewhat less common electron channel barrier. Barrier formation in the electron channel is even more sensitive to the alignment of the various gradients making up the sheared radial electric field then the ion barrier is. Electron channel heat transport is found to significantly increase after the formation of the ion channel barrier but before the electron channel barrier is formed. This increased transport is important in the barrier evolution.

PACS numbers: 52.25.Fi, 52.55.Dy, 52.35.Ra

* Research sponsored by the Office of Fusion Energy, U.S. Department of Energy, under contract DE-FG03-00ER54599 with Univ. of Alaska and DE-AC05-00OR22725 with UT-Battelle, LLC

1. Introduction

One of the more important and exciting recent advances in the physics of confined plasmas has been the production and concomitant developing understanding of enhanced confinement regimes. If controllable, these operating regimes offer the promise of an easier path to the economic production of fusion energy. Over the last 10 years a wide variety of magnetic confinement devices have found transitions to such an enhanced confinement regime [1-8]. These regimes include edge transport barriers and internal transport barriers as well as combinations of both.

A simple model incorporating the nonlinear interactions between the low-k turbulent fluctuations and the sheared radial electric field coupled to a transport model has been able to capture much of the observed dynamics [9-11] of ion transport barriers and has even been able to suggest barrier control strategies. However, an open question that remains is the nature and dynamics of the active electron thermal transport channel which is sometimes observed in the presence of a standard ion channel barrier. An understanding of the electron channel is important not only because it can become the dominant energy flow channel when in the presence of an ion channel barrier, but also because in devices in which $T_e \geq T_i$ this channel is always important. This, of course, is likely to be the case for reactor relevant regimes. By adding to the simple model mentioned above an evolution equation for electron fluctuations, such as a simplified version of the electron temperature-gradient-driven turbulence model (ETG), one can investigate the interaction between the formation of the standard ion channel barrier and the somewhat less common electron channel barrier. While it has previously been found that the ion channel barrier is sensitive to the alignment of the various gradients that make up the sheared radial electric field, we now find that the barrier formation in the electron channel is even more sensitive. It should be remembered that these gradients include both the first and second derivatives of the temperature and density as well as the gradients of the toroidal and poloidal flows.

The sensitivity to the alignment of the various gradients has significant implications for operating scenarios in which barrier control plays an important part. It

also highlights the importance of having a variety of real time profile modification tools to facilitate the initiation of barrier formation and its subsequent control. The electron channel heat transport is found to significantly increase after the formation of the ion channel barrier but before the electron channel barrier is formed. This increased transport is important in the ion barrier evolution, the electron barrier initiation and the final "steady state" profiles if an electron barrier does not form.

The rest of the paper is organized as follows. In Sect. 2, we discuss the extension of the transition model to include the electron channel transport. The results on the formation and evolution of the transport barriers are presented in Sect. 3. Finally, in Sect. 4 we give the conclusions of this paper.

2. Extended Model for Internal Transport Barriers

The basic model for the ion transport barrier consists of a set of transport equations for the density (n), ion temperature (T_i) and electron temperature (T_e) plus a nonlinear dynamical envelope equation for the fluctuations (ε).

$$\frac{\partial n}{\partial t} = S_{NBI} + S_{gp} + \frac{1}{r}\frac{\partial}{\partial r}\left[rD_n \frac{\partial n}{\partial r} \right] \qquad (1)$$

$$\frac{3}{2}\frac{\partial nT_i}{\partial t} = \frac{1}{r}\frac{\partial}{\partial r}\left[r\left(\chi_i n \frac{\partial T_i}{\partial r} + \frac{5}{2} D_n T_i \frac{\partial n}{\partial r} \right) \right] - D_n \frac{1}{n}\frac{\partial n}{\partial r}\frac{\partial nT_i}{\partial r} + Q^i_{NBI} + Q_{ei}\left(T_e - T_i \right) \qquad (2)$$

$$\frac{3}{2}\frac{\partial nT_e}{\partial t} = \frac{1}{r}\frac{\partial}{\partial r}\left[r\left(\chi_e n \frac{\partial T_e}{\partial r} + \frac{5}{2} D_n T_e \frac{\partial n}{\partial r} \right) \right] + D_n \frac{1}{n}\frac{\partial n}{\partial r}\frac{\partial nT_i}{\partial r} + Q^e_{NBI} + Q_{Ohm} + Q_{ie}\left(T_e - T_i \right) \qquad (3)$$

$$\frac{\partial \varepsilon}{\partial t} = \left\{ \gamma - \alpha_1 \varepsilon - \alpha_2 \left[\frac{r}{q}\frac{\partial}{\partial r}\left(\frac{q}{r}\frac{E_r}{B_\varphi} \right) \right]^2 \right\} \varepsilon + \frac{1}{r}\frac{\partial}{\partial r}\left[rD_\varepsilon \frac{\partial \varepsilon}{\partial r} \right] \qquad (4)$$

The fluctuation evolution equation is coupled to the transport equations in two ways. First, through the transport coefficients, which are defined in the following way $\chi_i \equiv \chi_{in} + \chi_{i0}\varepsilon^2$ with similar forms for the other coefficients. Secondly, the density and temperature profiles couple to the fluctuations through the radial electric field via the

force balance equation,

$$E_r = -V_\theta + V_\phi \frac{B_\theta}{B_0} + \alpha \left[\frac{\partial T_i}{\partial r} + \frac{T_i}{n} \frac{\partial n}{\partial r} \right] \tag{5}$$

This five equation model and many of its features are explained in detail in refs [9] and [10]. Here, we will give a brief overview of some of the terms.

The growth rate γ in the fluctuation equation, Eq. (3), is based on the toroidal η_i model of Biglari el al [12]. It includes a term responsible for magnetic shear stabilization as well as the more self-consistent profile related form common to ion temperature gradient driven turbulence models (ITG). The magnetic shear component is important for internal transport barrier investigations as we do not evolve current profiles in this model. The fluctuations in turn dynamically adjust the profiles through the D and χ terms in the transport equations. Finally, the fluctuation equation is coupled a second time to the profiles through the radial electric field. This is via the third term on the right hand side of the fluctuation equation. This suppression term is of the Hahm Burrell form [13] and it is very important for the dynamics that the electric field shear has all of the pressure gradient terms as well as the velocity gradient terms. The model has evolution equations for the poloidal and toroidal flows however, for simplicity, in this paper we have not included them. All of the coefficients in the model are described in detail in ref [9].

In order to investigate the electron channel, we add one equation to this basic model. We now include an evolution equation for the envelop of the electron scale fluctuations (ε_e),

$$\frac{\partial \varepsilon_e}{\partial t} = \left[\gamma_e - \alpha_{1e} \varepsilon_e - \alpha_{2e} \left(\frac{r}{q} \frac{\partial}{\partial r} \left(\frac{q}{r} \frac{E_r}{B_\phi} \right)^2 \right) \right] \varepsilon_e + \frac{1}{r} \frac{\partial}{\partial r} \left[r D_{\varepsilon e} \frac{\partial \varepsilon_e}{\partial r} \right] \tag{6}$$

This equation has a form identical to that of the ion scale fluctuation equation however the various coefficients are changed to those for an electron scale turbulence model. For this paper we use an ETG model however the basic idea is valid with the model of your choice with only the growth rate and other coefficients changing. For the

ETG model we replace the ion temperature with the electron temperature in the appropriate places and most importantly change α_{2e} and χ_e.

The coefficient in front of the shear suppression term in Eq. (6) is reduced by the ratio of the mean turbulent wavenumbers for electron and ions. This is because a larger shear is required to suppress smaller scale fluctuations. For this paper the ratio is taken to be between 20 and 100 (though once again the exact number is not essential to these results). The electron temperature equation is also modified through χ_e, which has a term with the same form as the ion fluctuation level term but now proportional to the electron fluctuation level squared added to it. This term is however reduced from the ion fluctuation level term by the ratio of the mean wavenumbers because of the reduced step size intrinsic to the smaller scale fluctuations.

In this paper we used the values shown in Table 1 as typical parameter values for the calculations. It should be noted that the details of these values are not important, as the overall behavior is very insensitive to these specifics.

3. Barrier Formation and Evolution

Using the model described in Sect. 2, we have carried out a sequence of calculations for different values of the total power absorbed and different widths of the power deposition profiles. The later is crucial in controlling the evolution of the transport barriers. A broad central beam deposition profile (shown in Figure 1a) can lead to a narrow ion channel transport barrier as seen in the reduction of the transport coefficients (Figure 2a circles) due to the decreased flux through a given radial location relative to a narrow deposition profile with the same power. With a narrow deposition profile (Figure 1b) the converse is true and a broad barrier in the ion channel can form (Figure 2a squares). It should be noted that the transport coefficients shown in Figure 2a are time averaged. They come from instantaneous profiles that exhibit propagating oscillations in the barrier region. These oscillations can have a much larger effect in the reduction in the transport (Figure 2b). These oscillations are physically based and have been investigated in reference [10]. However, while physical, the waves propagate further then they physically should because an envelope turbulence model such as the one used here cannot have real turbulent decorrelation. Near the critical transition power this then leads to a smaller average reduction in the transport coefficient.

This is particularly true with the narrow barrier through which these waves can easily pass.

In general, initial formation of the ion channel barriers is facilitated by a narrower deposition profile (for a fixed total power) because of the larger flux through the critical radial surface. However after the ion channel barrier is formed, the width of the barrier is instrumental in setting the profile shape and in turn, this barrier width is determined in part by the beam deposition profile. Inside the actual barrier the profile is flatter both because of the larger transport as well as a small power amount of power deposited in that region. In the case of the narrow barrier (broader deposition profile) the second derivative of the pressure profile constituents is usually found to be larger at the top and bottom of the barrier region then in the case of the broad barrier (narrow deposition profile) (Fig 4b vs Fig. 3).

When the evolution equation for electron fluctuations is added, the details of the post ion channel transition profiles become important. As shown above, the narrow barrier in the ion channel leads to a sharper change (second derivative) in the temperature and density profiles, which in turn can lead to a well–aligned and large gradient in the radial electric field. This in turn can lead to a barrier forming in the electron channel. Formation of this barrier requires a larger radial field shear due to the higher k involved in the fluctuations. With the broader ion channel barrier (from the narrow deposition profile) the less sharp profile features leads to a higher power threshold for the electron channel barrier. In the case of the narrow deposition profile a broad peaked barrier in the ion channel can form at lower power (Fig. 3) while still having an active electron channel.

Before an electron channel barrier forms (or in cases that only an ion barrier forms) the increased gradients leads to an increase in the electron fluctuation level (Fig. 4a). This increase can partially compensate for the reduced (or eliminated) transport in the ion channel. The increase in the electron scale fluctuations therefore can cause a local decrease in the slope of the T_e profile (Fig. 4b) which can prevent the formation of the electron barrier at the footpoint of the ion channel barrier.

When an electron barrier does form, it tends to form near the steep curvature region at the top of the ion barrier (Fig. 5) and can grow outward from there. This is also

just inside the region of increased fluctuation level in the electron channel fluctuations, see for example just outside $r/a = 0.2$ in Fig. 4a. The increased fluctuation level, which causes the flattening of the slope, also enhances the curvature (the second derivative) of the profile just inside that point helping to facilitate the initiation. For all of the cases studied with this model, the electron barrier footpoint remains inside the ion barrier footpoint.

The formation and evolution of an electron transport channel barrier in the presence of an ion transport channel barrier allows for very complex dynamics. Oscillations often found at the transition point [10] now can have multiple characteristic frequencies that can also interact either helping or hindering the barrier propagation depending on their amplitude. The propagation of these oscillations changes and the oscillations themselves can become less regular (Figure 6). In Figure 6, the ion barrier can be seen to extend out to approximately r/a of .4 while the electron barrier extends from r/a of 0.2 to 0.25. These profiles are the instantaneous fluctuation levels and the irregular propagating oscillations can be seen in both fields.

This complex interrelated dynamics between the two channels allows for a number of potential control schemes such as utilizing the electron channel as a profile control valve. Because the underlying physics of both barriers is based on an interplay between fluctuation growth mechanisms and shearing suppression effects, it has been shown that various mechanisms can lead to same result and trigger the transition. This is potentially useful as it provides for the possibility of many tools for both initiation and control. The underlying tools need only modify either E_r' or local growth rate or both, hence these only need to be local profile modification tools. Some possible tools for this include local heating, forced H–L transition (or other edge collapse), pellet injection, toroidal or poloidal flow modification (including modification of zonal flows). Because the electron channel barrier tends to be narrower and somewhat less robust, it might offer a control channel for relaxation of the confinement. Due to the less robust nature and the narrower width this might be accomplished with moderate powers through transient local current profile modifications.

4. Conclusions

Using the relatively simple model proposed here, one can investigate the interaction between the formation of the standard ion channel barrier and the somewhat less common electron channel barrier. The transport barrier formation in the electron channel is found to be even more sensitive to the alignment of the various gradients making up the sheared radial electric field then the ion barrier is.

Power deposition profiles are important in setting up the transport barriers. A reason is that the curvature of the profiles is also an important contributor to the shear in the radial electric field. Broader power deposition profiles facilitate the formation of the electron channel barrier.

After the formation of the ion channel barrier but before the electron channel barrier is formed, the electron channel heat transport is found to significantly increase. This increased transport is critical to both the ion barrier evolution and to the initiation and formation of the electron channel barrier.

This simple model by including a dynamically evolving set of coupled transport and fluctuation equations allows one to investigate the parameters that lead to optimal performance regimes. Transport barrier control scenarios will be investigated in future work.

References

[1] Y. Koide, et al., Phys. Rev. Lett. **72**, 3662 1994.

[2] B. LeBlanc et al., Phys. Plasmas **2**, 741 1995.

[3] M. Greenwald, et al., Phys. Rev. Lett. **53**, 352 1984.

[4] F. Wagner, et al., Phys. Rev. Lett. **49**, 1408 1982.

[5] F. M. Levinton, et al., Phys. Rev. Lett. **75**, 4417 1995.

[6] E. J. Strait, et al., Phys. Rev. Lett. **75**, 4421 1995.

[7] E. A. Lazarus, et al., Phys. Rev. Lett. **77**, 2714 1996.

[8] Y. Koide and JT-60 Team, Phys. Plasmas **4**, 1623 1997.

[9] D. E. Newman, B. A. Carreras, D. Lopez-Bruna, P. H. Diamond, and V. B. Lebedev, Phys. Plasmas **5,** 938 (1998).

[10] D. Lopez-Bruna, D. E. Newman, B. A. Carreras, and P. H. Diamond, Phys. Plasmas **6**, 854 (1999).

[11] E. J. Synakowski, et al, Nucl. Fusion **39**, 1733 1999.

[12] H. Biglari, P. H. Diamond, and P. W. Terry, Phys. Fluids B **2**, 1 (1990).

[13] T. S. Hahm and K. H. Burrell, Phys. Plasmas **2**, 1648 1995.

Table 1. Typical parameters used for the calculations presented

Parameter	**Value**
B_0	90000 gauss
Major radius (R)	150 cm
Minor radius (a)	42 cm
Total Beam power	5-14 MW
Beam 1(central) deposition half width	0.15 - 0.35a
Beam 2 deposition center	0.2a
Beam 2 power fraction	0.0-0.2
Beam 2 deposition half width	0.2a
Shear parameter (α_2)	0.1-0.2

Figure captions

Fig. 1. Integrated power for two deposition profiles each with the same total power. a) A broad deposition profile leads to only half the total power through $r/a = 0.35$ while b) a narrow deposition profile leads to almost the total power through $r/a = 0.35$.

Fig. 2. Thermal transport coefficients from η_i fluctuations for a) the ratio of barrier to no barrier time averaged coefficients with the broad deposition profile showing narrow barrier (circles) and the narrow deposition profile showing broad barrier (squares) b) three instantaneous profiles showing the wave like oscillations (see Fig 6) that can occur and the instantaneous many order of magnitude reduction in the transport coefficients and neoclassical component.

Fig. 3. Temperature profiles after an ion channel barrier forms from a narrow deposition profile

Fig. 4. a) η_e fluctuation level increases after ion channel barrier forms but before electron channel barrier forms b) Temperature profiles showing a flattened region in the electron temperature profile and a broader flat core due to a broader deposition profile

Fig. 5. a) η_e and η_i fluctuation levels showing both ion and electron channel barriers in a broad deposition profile case with the electron barrier forming near strong curvature region at the top of the ion barrier. b) Temperature profiles showing a steepened region in the electron temperature profile, inside the ion barrier foot point and a broader flat core due to the broad deposition profile

Fig. 6. η_e and η_i instantaneous fluctuation levels showing both ion and electron channel barriers in a broad deposition profile case with the electron barrier forming near strong curvature region at the top of the ion barrier. Irregular oscillations can be seen in both fields around the barrier regions.

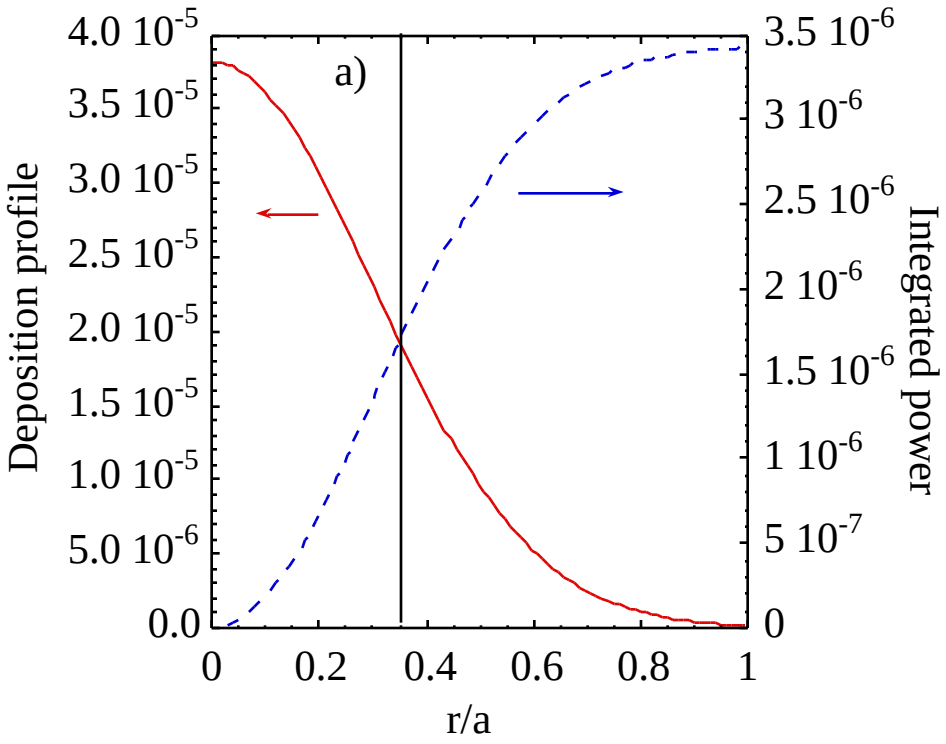
a)
Deposition profile
Integrated power
r/a
4.0 10-5
3.5 10-5
3.0 10-5
2.5 10-5
2.0 10-5
1.5 10-5
1.0 10-5
5.0 10-6
0.0
3.5 10-6
3 10-6
2.5 10-6
2 10-6
1.5 10-6
1 10-6
5 10-7
0
0
0.2
0.4
0.6
0.8
1

Fig. 1a

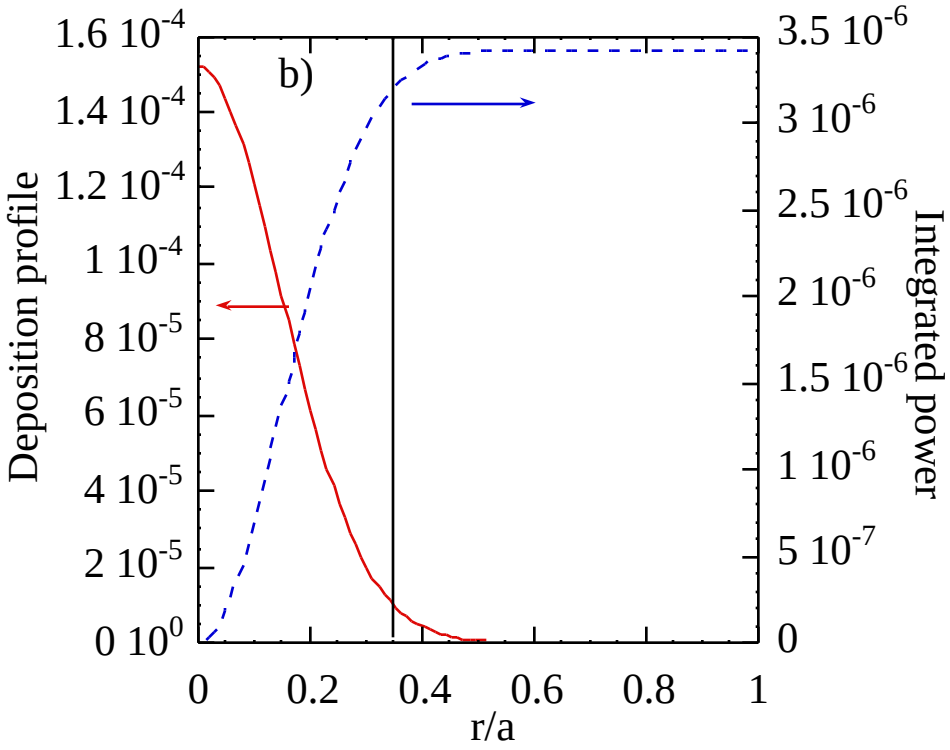
b)
Deposition profile
Integrated power
r/a
1.6 10-4
1.4 10-4
1.2 10-4
1 10-4
8 10-5
6 10-5
4 10-5
2 10-5
0 100
3.5 10-6
3 10-6
2.5 10-6
2 10-6
1.5 10-6
1 10-6
5 10-7
0
0
0.2
0.4
0.6
0.8
1

Fig. 1b

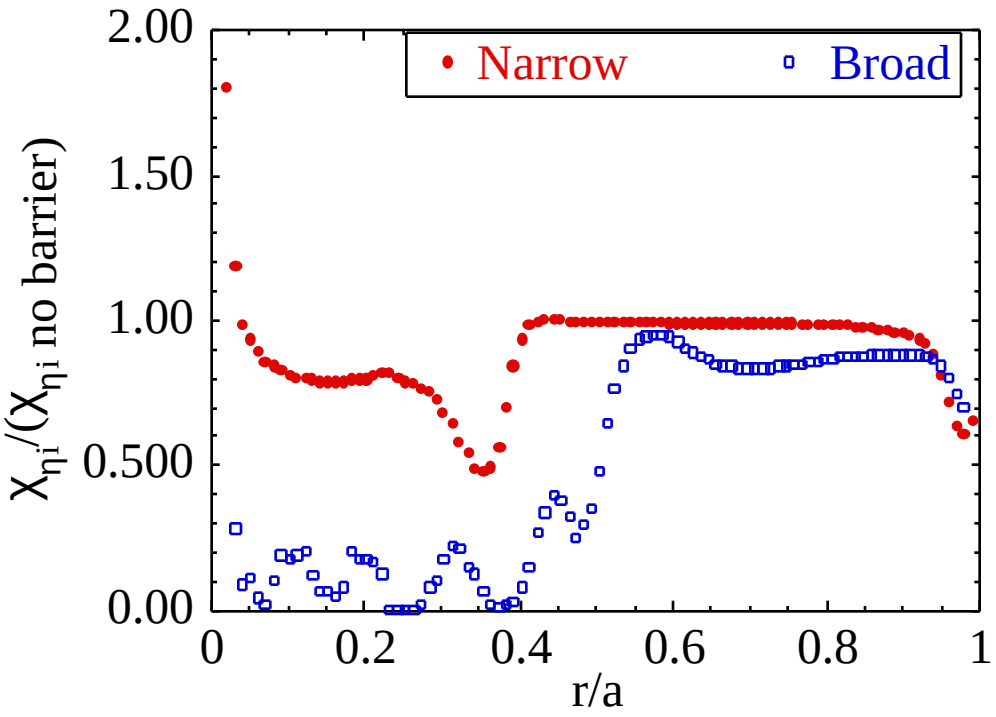
2.00
1.50
1.00
0.500
0.00
0
0.2
0.4
0.6
0.8
1
r/a
$\chi_{\eta i}/(\chi_{\eta i}$ no barrier)
Narrow
Broad

Fig. 2a

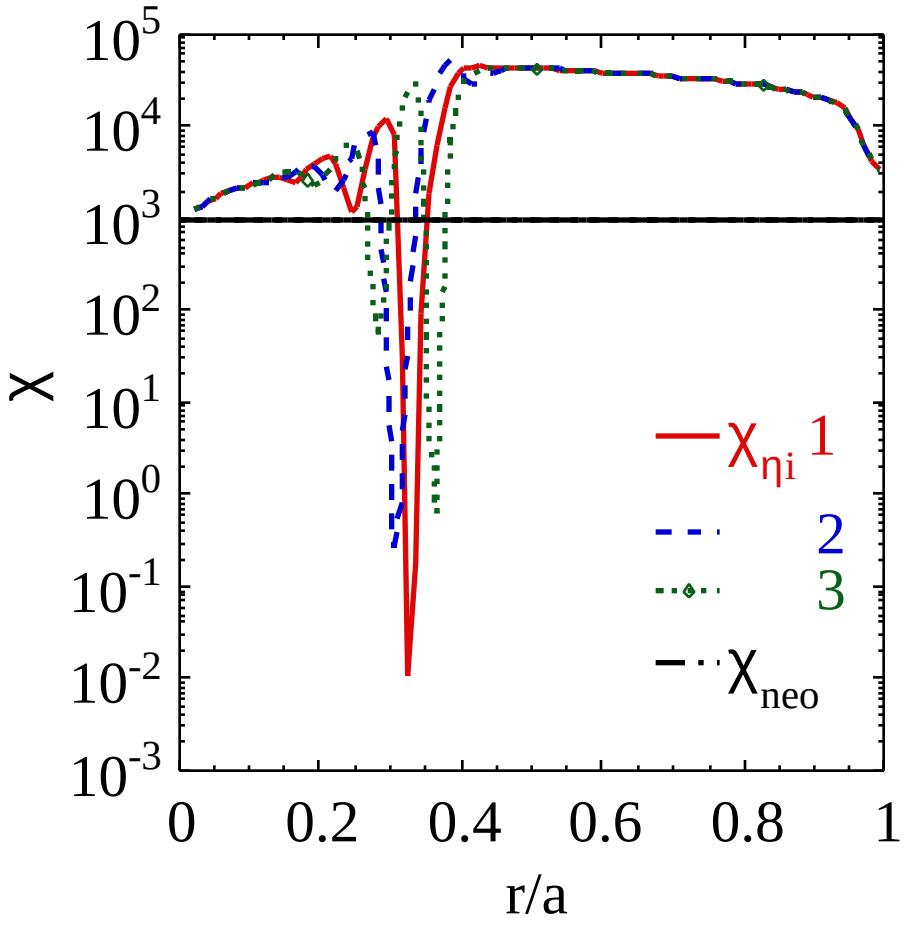
10^5
10^4
10^3
10^2
10^1
10^0
10^{-1}
10^{-2}
10^{-3}
χ
0
0.2
0.4
0.6
0.8
1
r/a
$\chi_{\eta i}$ 1
2
3
χ_{neo}

Fig. 2b

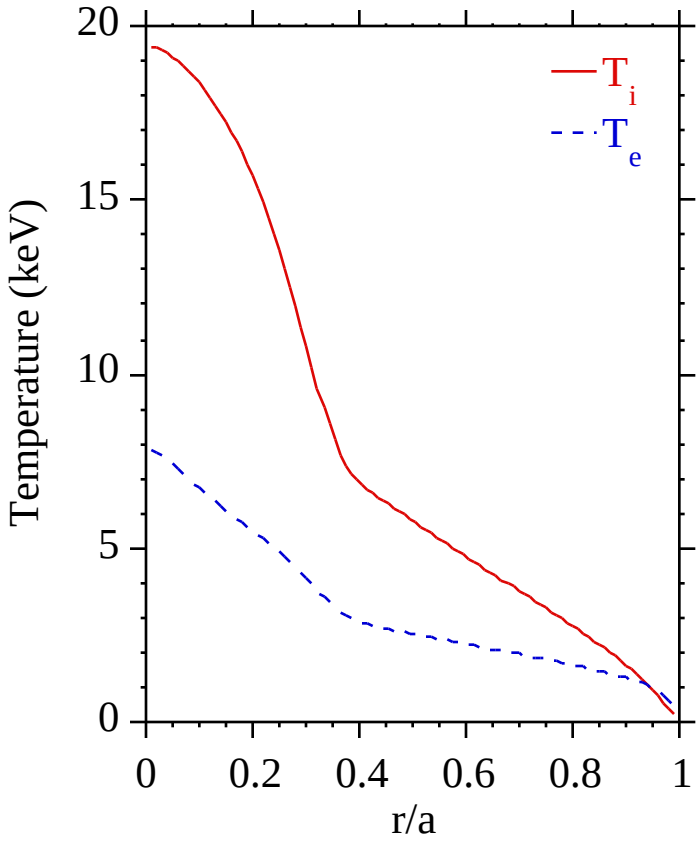

Fig. 3

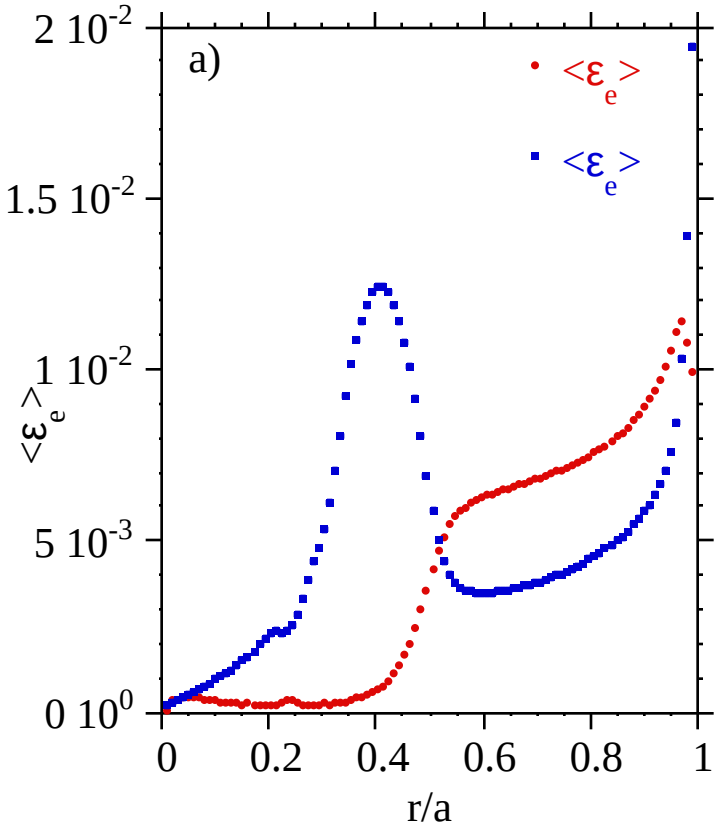

Fig. 4a

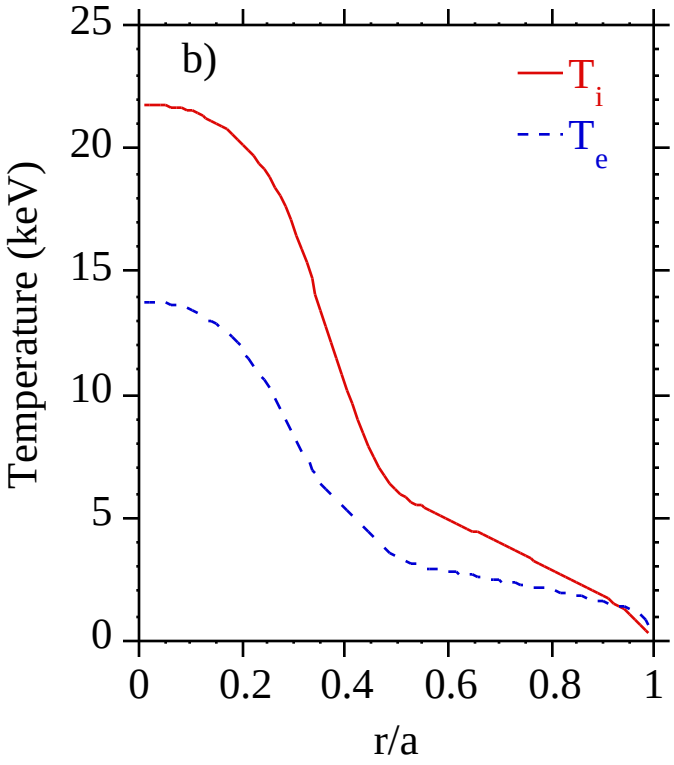

Fig. 4b

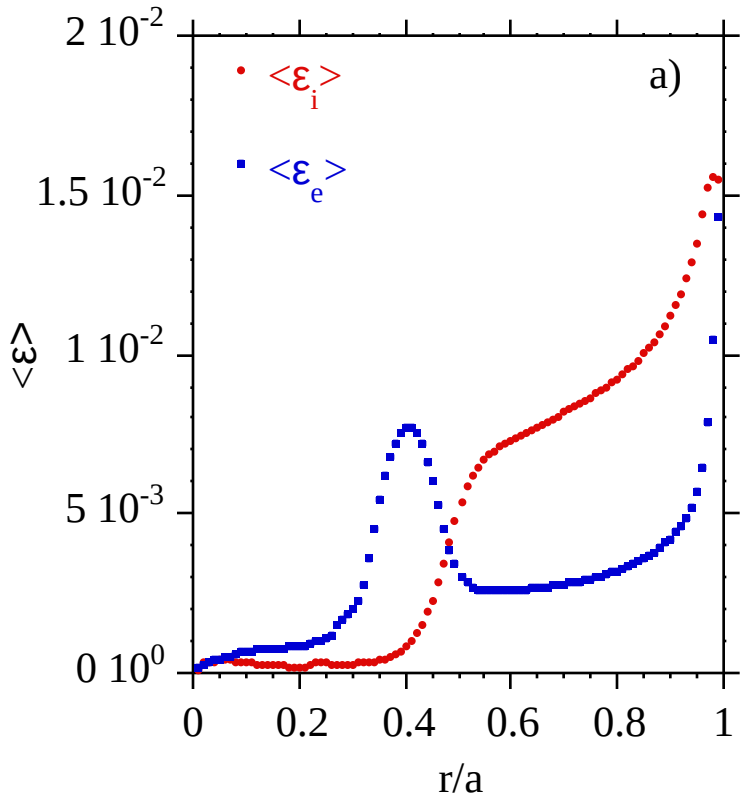

Fig. 5a

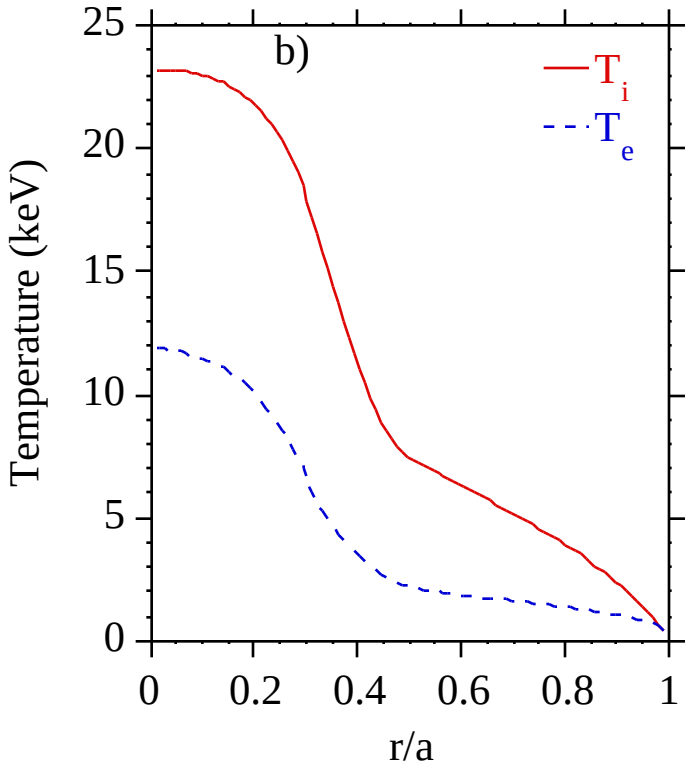

Fig. 5b

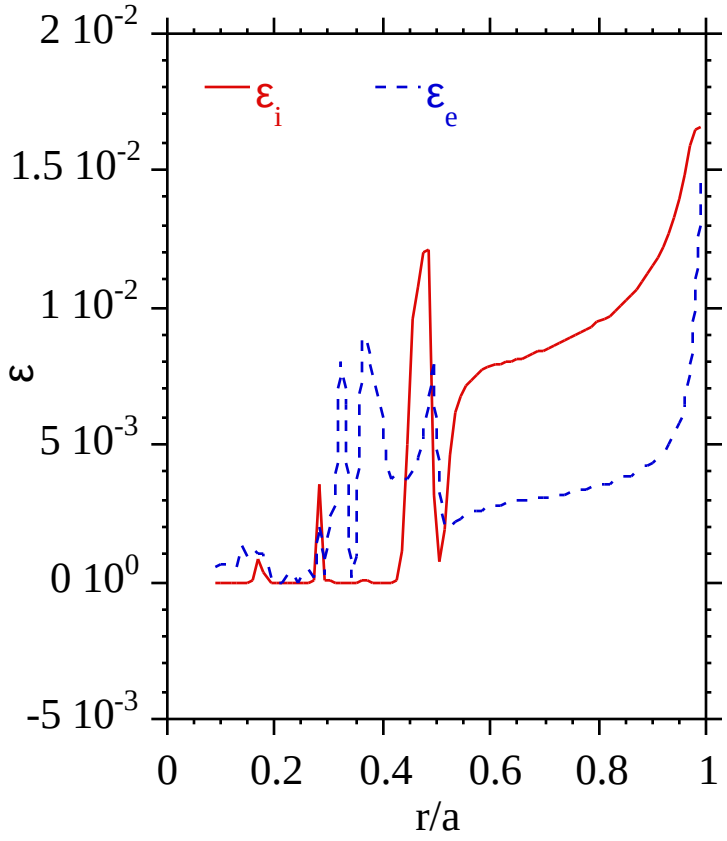

Fig. 6